Consolidated Technical Specifications for the Advanced Pedestrian Legform Impactor (aPLI)

Takahiro Isshiki, Jacobo Antona-Makoshi, Atsuhiro Konosu, Yukou Takahashi

Abstract This study aims to consolidate the final technical specifications of the Advanced Pedestrian Legform Impactor by expanding the biofidelity evaluation of its finite element model. The biofidelity evaluation is expanded by employing an existing set of post-mortem human subject lateral impact tests and with a set of human body model lateral and oblique impact simulations. Initial comparisons of the biomechanical response obtained from previous legform-impactor computational models revealed that the impactors sustained greater bumper and spoiler contact forces than the post-mortem human subjects in experiments. Moreover, they sustained greater cruciate ligament elongations than the human body models in the oblique impact simulations. The Advanced Pedestrian Legform Impactor model includes a more human-like lower-limb mass distribution and a redesigned geometry for the femoral condyle of the knee; the biofidelity and the injury assessment capability of the model were thus re-evaluated. The mass distribution modifications contributed to the improvement of the contact force responses at various car front-end components compared with those obtained from the lateral impacts using post-mortem human subjects. The structural redesign of the knee enhanced the performance of the injury measurements in the simulated oblique impacts. The present study shows that the Advanced Pedestrian Legform Impactor presents improvement in the performance of previous impactors for a wide range of vehicle front-end characteristics, including bumper height and bumper orientation.

Keywords bumper corner, legform impactor, lower-limb injuries, pedestrian safety.

I. INTRODUCTION

The lower limb is the most frequently injured body region in car-to-pedestrian accidents globally [1-2], accounting for 43%, 35%, and 37% of all serious injuries sustained by pedestrians in the US and Germany in 2012 [3] and in Japan in 2015 [4], respectively. Lower-limb injuries sustained by pedestrians cause significant harm to society and must be prevented. The front-end design characteristics of a vehicle are relative to the height and location of pedestrians and are highly correlated with the in-crash kinematics and injury probability of pedestrians. Low-bumper cars tend to be more associated with leg and knee injuries, whereas high-bumper cars tend to be more associated with femoral fractures [5]. Lower-limb injuries are most commonly caused when pedestrians are hit laterally by the central part of the front end of a vehicle [3]; however, a significant amount of impacts with bumper corners that tend to have angulated surfaces have been reported as well [6]. Serious lower-limb injuries sustained by pedestrians most commonly include long-bone (femur, tibia, and fibula) fractures; nevertheless, knee-ligament and ankle injuries are often reported as well [7].

One common approach for the prevention of pedestrian lower-limb injuries is the evaluation of the safety performance of various car front-ends through standardised impact tests using legform impactors (UN regulations, New Car Assessment Programs (NCAPs)). For this purpose, the Advanced Pedestrian Legform Impactor (aPLI) has been recently developed [8-11]. The aPLI incorporates a number of enhancements for improved lower-limb injury prediction compared with its predecessor, the Flexible Pedestrian Legform Impactor (FlexPLI). The aPLI incorporates a Simplified Upper-Body Part (SUBP) connected to the lower limb by a cylindrical mechanical hip joint. The combination of the SUBP and the joint simulates the effect that the upper body has on the lower limb in crash kinematics and kinetics for a wide range of vehicle front-end characteristics; this enhances the suitability of the impactor to evaluate pedestrian lower-limb injury risk in impacts with both low- and high-bumper cars [11]. Throughout the development of the aPLI, the effect of a large number of design parameters on its biofidelity was computationally optimised by means of response surface methodology [10];

the structural design of the aPLI was simplified to improve its repeatability and reproducibility without affecting its biofidelity [11]. Previous work on the aPLI has shown its great potential as a tool for the evaluation of lower-limb injury probability in pedestrian lateral impacts.

Despite the previous promising results, the aPLI validations that have been conducted thus far have been focused on evaluating injury assessment capability using a thoroughly validated 50th percentile male (50M) human body model (HBM) in 40 km/h impact simulations. The impacts were delivered using vehicle front-end configurations that represented the central bumper parts. This evaluation process has two main limitations. First, the response of the aPLI has not been directly compared with experimental data from a full-scale post-mortem human subject (PMHS); this limitation can now be addressed with PMHS corridors that have recently become available [12-13]. Second, the performance of the aPLI in impacts with bumper-corner areas that had pronounced angles was unknown; this requires additional comparisons with HBMs in oblique impacts. The importance of addressing the aforementioned bumper-corner areas is illustrated by the fact that they may become incorporated into UN regulations [14].

The long-term goal of this study is to contribute to the minimisation of lower-limb injuries in pedestrians when hit by the frontal part of cars, regardless of the bumper height or the location of the bumper lateral impact. More specifically, the aim is to consolidate the final technical specifications of the aPLI by expanding its computational biofidelity evaluation using an existing set of PMHS lateral-impact test corridors and its injury assessment capability using a new set of HBM oblique and lateral impact simulations.

II. METHODS

A two-step approach was followed in this study. First, the original aPLI model—which was developed in a previous study [11]—was updated to enhance its biofidelity by comparing the aPLI data with the PMHS experimental data [12] and to strengthen its injury assessment capability by comparing aPLI data with HBM oblique impact simulation data (hereafter referred to as the modified aPLI model). The modifications were preliminarily validated through a limited range of representative impact scenarios by comparing the responses of both the original and the modified aPLI models with the responses of full-scale PMHS lateral impact experiments [12] and HBM lateral and oblique impact simulations, respectively. Second, three finite element (FE) models of the legform impactor (hereafter referred to as FlexPLI model, FlexPLI+SUBP model, and Modified aPLI model) were evaluated by comparing their kinematics and injury measures responses with the responses of full-scale PMHS lateral impact experiments [12] and those of the HBM lateral and oblique impact simulations, respectively, for a wider range of impact scenarios. The descriptions of the FE impactor models and the methodologies that were applied to objectively evaluate their responses will be presented in the following sections. All simulations presented in this study were executed using the PAM-CRASH software package (ESI, Paris, France).

Legform Impactor Finite Element Models

The top row in Fig. 1 illustrates an HBM and the legform impactor models. The FlexPLI model was adopted from a previous study [15]; it has been described in detail and has been applied in several studies [16-17]. The original aPLI model consisted of a SUBP and a hip joint (Fig. A15, Appendix A) [10] that was connected to a mechanical lower limb. The design characteristics of the lower limb evolved from the FlexPLI; its effect on the injury measures has been previously verified through several numerical studies [8-11]. The aforementioned evolved and verified characteristics included a relative flesh-to-bone mass distribution that was closer to that of humans, an increased femoral bending stiffness that was achieved by manufacturing a thicker mechanical femoral bone core, long-bone human-like contours on the impact side, and a geometry of the cruciate knee ligaments in the sagittal plane that was closer to that of humans and of the HBM (Fig. 1, middle row). Additionally, in the present study, two new structural modifications were incorporated into the original aPLI model to develop the modified aPLI model. First, the mass distribution of five sections along the mechanical

Takahiro Isshiki (phone: +81-29-856-0885, e-mail: tissiki@jari.or.jp), Jacobo Antona-Makoshi and Atushiro Konosu are researchers at the Japan Automobile Research Institute, Tsukuba, Japan. Yukou Takahashi is chairperson of pedestrian safety experts group at the Japan Automobile Manufacturers Association, Inc., Tokyo, Japan.

lower limb was modified by adjusting the density of the surrounding flesh to match the mass of each section with the corresponding sections in the HBM as much as possible (Fig. 1, top row). This modification was implemented based on the assumption that a more human-like mass distribution would help to refine the balance of the forces that are transferred between the impactor and the different components of the car front-end. The modification was facilitated by the fact that contact force corridors for these components have become available [12]. In addition, the modification was supported by a previous study on aPLI optimisation, in which it was revealed that if the mass distribution along the aPLI mechanical lower limb was more akin to that of humans, the correlation between the injury measurements from the impactor and those from the HBM would be higher [10]. The second structural modification that was incorporated to the aPLI pertained to the knee and involved the redesign of the shape of the femoral condyle of the knee (highlighted in yellow in the middle row, Fig. 1). The original shape of the femoral condyle was nearly parallelepiped, which was modified to have a nearly ellipsoidal shape. The purpose of this modification was to achieve the human-like relative motion between the femoral condyles and the meniscus that can be expected in oblique lateral impacts. Finally, the FlexPLI+SUBP model was developed by connecting the SUBP to the former FlexPLI via the aforementioned mechanical cylindrical joint (Fig. A16, Appendix A). This impactor was included to investigate the isolated contribution to the lower-injury indicators of the SUBP and of the aPLI's lower-limb modifications, respectively.

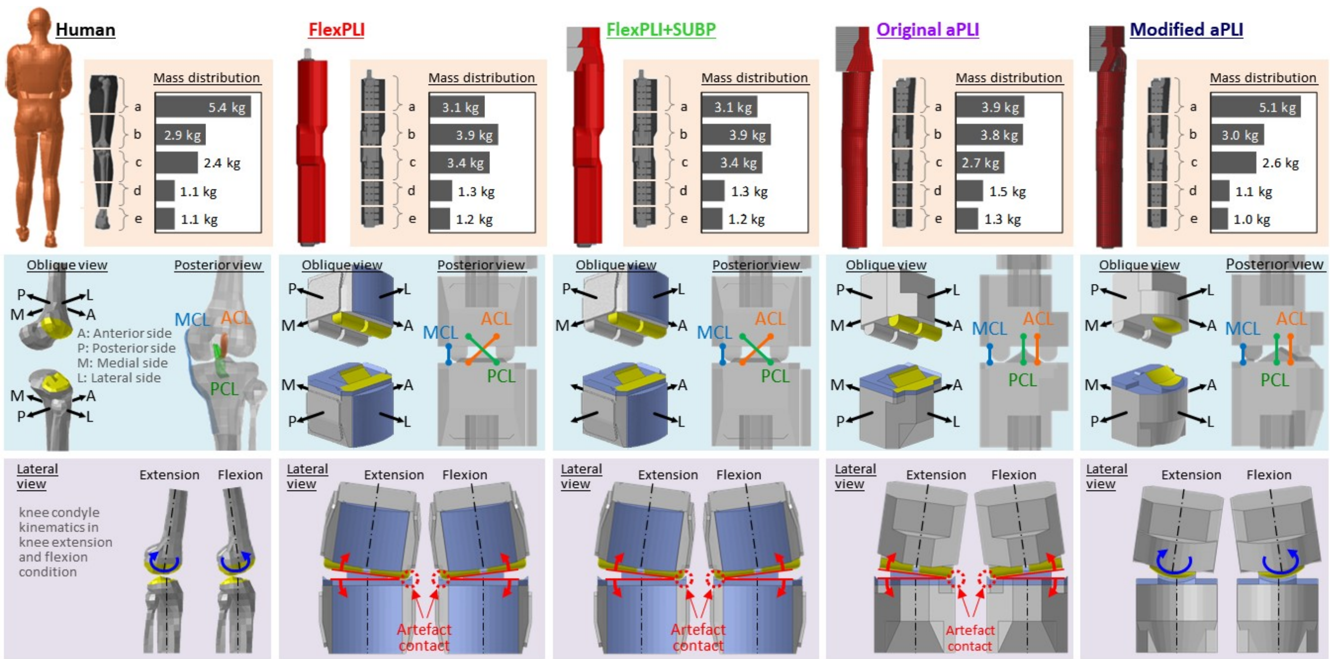

Fig. 1. Top row: Posterior view of the HBM and of the legform impactor models that are evaluated in the present study, including the mass distribution in five sections along the lower limb of the models. Middle row: oblique and posterior views of the HBM knee and of the legform impactor models. The images of the posterior view include a sketch of the medial collateral ligament (MCL), the anterior cruciate ligament (ACL), and the posterior cruciate ligament (PCL) of the knee. Bottom row: Knee condyle kinematics in knee extension and knee flexion.

Biofidelity Evaluation with PMHS Lateral Impact Tests

Kinematics and contact-force corridors that have been recently developed from PMHS impact experiments [12] were adopted in the present study. The experiments comprised 11 PMHSs in mid-gait stance that were impacted laterally at 40 km/h by a modular generic buck [12]. The buck was composed of four components: two cylindrical tubes that were screwed on rigid supports, which represented the bumper (BP) and the spoiler (SP), respectively; a quarter of a steel cylindrical tube, which represented the bonnet leading edge (BLE); and a steel plate, which represented the bonnet. The relative layout of these components was varied to represent the front-end geometry of a Sedan, a Sport-Utility Vehicle (SUV), and a Van. The contact forces between each of the components and the lower extremities of the specimens were recorded via load cells placed behind each component. The in-crash kinematics of the specimens was captured via photo targets and high-speed videos. The recorded data were scaled to a M50 size and used for the development of BP, SP, and BLE force corridors, as well as for full-body trajectory corridors for each of the three vehicle types [12].

In the current study, the FE models of the three generic bucks used in the PMHS experiments were developed according to the technical specifications described in the original publication [12]. For the first step, two legform impactor models (Original aPLI and Modified aPLI, Fig. 1) were applied for the simulation of an impact with a generic Sedan buck model to preliminarily confirm the effect of the modified mass distribution on the impact forces. After the preliminary evaluation, each of the three legform impactor models (FlexPLI, FlexPLI+SUBP, and Modified aPLI, Fig. 1) was applied to the simulation of an impact with each of the three generic buck models; in total, nine simulations were executed. The responses of the knee and ankle displacements and the contact forces between the impactors and the buck components were extracted from the simulations with the legform impactor models; next, they were compared with the corresponding corridors from the experiments. The CORA method was applied for the objective evaluation of these comparisons [18].

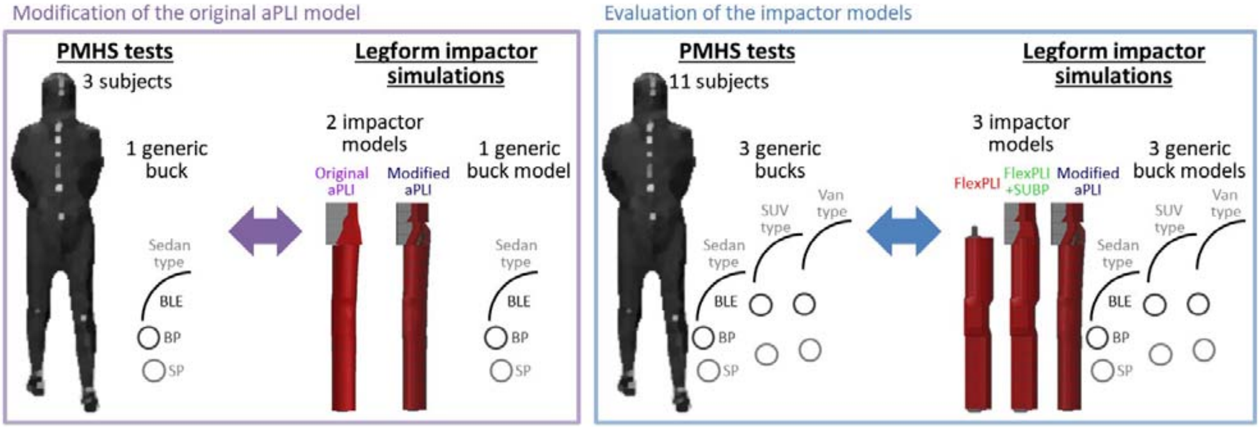

Fig. 2. Left: schematic of the PMHS lateral impact tests, including a sketch of the lateral profile of the BLE, BP, and SP components for the configuration of the generic Sedan buck; schematic of the two legform impactor models and the buck model applied for the simulation of lateral impacts that are similar to the experiments for the initial validation of the modified aPLI. Right: schematic of the PMHS lateral impact tests, including a sketch of the lateral profile of the BLE, BP, and SP components for the configurations of the generic Sedan, SUV, and Van buck; schematic of the three legform impactor models and the buck models applied for the simulation of lateral impacts that are similar to the experiments for the second validation of the modified aPLI.

Evaluation of the Injury Assessment Capability with HBM Lateral and Oblique Impact Simulations

An HBM that had been previously validated at component- and full-scale levels [5][19-21] and a set of 36 simplified car front-end models from a previous aPLI work [11][22] were incorporated into the present study. Details on the HBM validation and on the simplified car models are presented in Appendices B and C, respectively. In the present study, for the preliminary evaluation step, the HBM and each of the two impactor models were applied for the simulation of the impacts with two different simplified car front-end models (Sedan 09 and SUV 15 in Table C2 in Appendix C) under two horizontal angulations, totalling four HBM simulations and eight legform impactor model simulations (Fig. 3, top row). Each of the two horizontal angulations represented the left bumper corner area, with an angle of 40° (L40), and the central bumper area, with an angle of 0°. These choices were aimed at the evaluation of the modified condyle shape of the knee under oblique impact conditions, particularly regarding the ACL elongation response. The angle of 40° for the oblique impacts was selected based on the requirement issued in the UN-R127-02 series amendment regulation, which stipulates that bumper corner angles greater than 30° be investigated [14]. After the preliminary evaluation, the HBM and each of the three impactor models were employed for the simulation of series of impacts with the 36 simplified car front-end models under three horizontal angulations, totalling 108 HBM simulations and 324 legform impactor simulations (Fig. 3, bottom row). The three horizontal angulations were designed to represent the L40 configuration, the central bumper area with an angle of 0°, and the right bumper corner area with an angle of 40° (R40). For each impactor model, the simulated responses for a number of injury measures (i.e., thigh bending moment at three locations, leg bending moments at four locations, and MCL, ACL, and PCL elongations) were compared with the corresponding responses obtained via the HBM using the CORA method [18].

Thereafter, linear regression was applied between the peak values of the injury measurements from the impactors and those from the HBM to quantify the capability of the impactors to assess injuries as predicted with the validated HBM over a wide range of simulated impact conditions.

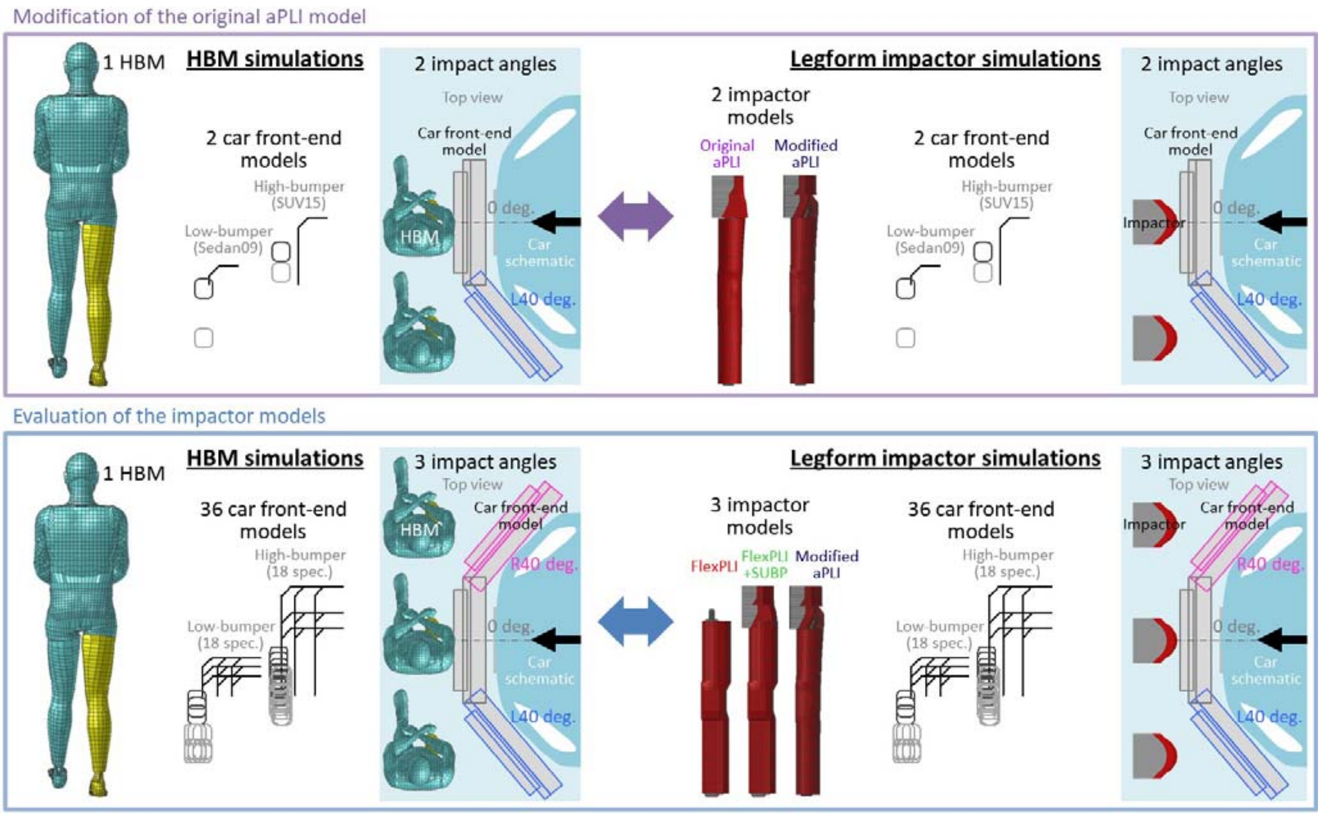

Fig. 3. Top: schematic of the HBM lateral and oblique impact tests, including a sketch of the lateral profile of the BLE, BP, and SP components for the two simplified car front-end models (e.g., Sedan 09 and SUV 15) and sketches of two impact angles; schematic of the impactor models that were used for the impact simulations that were conducted under the same impact conditions as those of the HBM simulations for the initial validation of the Modified aPLI. Bottom: schematic of the HBM lateral and oblique impact tests, including a sketch of the lateral profile of the BLE, BP, and SP components for the 36 simplified car front-end models and sketches of three impact angles; schematic of the impactor models that were used for impact simulations that were conducted under the same impact conditions as those of the HBM simulations.

III. RESULTS

In this section, the results obtained from the biofidelity evaluation using the PMHS test data will be presented, followed by the results corresponding to the evaluation of the injury assessment capability using the HBM simulation data.

Biofidelity Evaluation via the PMHS Lateral Impact Tests

Fig. D18 in Appendix D shows a comparison between the impact forces of the lower extremities of the PMHS and those of the two different impactors (i.e., Original aPLI and Modified aPLI). These simulations were conducted using the Sedan buck configuration to evaluate the effect of the modification of the mass distribution on the response of the impactors. In general, the Modified aPLI generates impact forces that are closer to those of the PMHS, thereby confirming the validity of the mass distribution modification.

Fig. 4 shows a comparison between the lower-extremity kinematics of the PMHS and the response of three different impactors (i.e., FlexPLI, FlexPLI+SUBP, and Modified aPLI) obtained from simulations using Sedan, SUV, and Van buck configurations. In general, both the FlexPLI+SUBP model and the aPLI model demonstrate similar kinematics to those of the corresponding PMHS for all three buck configurations.

The PMHS corridors that were developed for the knee and ankle trajectory in the coronal plane of the specimens according to the buck type [12] are shown in Fig. E20 in Appendix E. In each sub-figure, the corresponding responses from the three legform impactors are presented with different colours (FlexPLI in red, FlexPLI+SUBP in green, and aPLI in blue). The knee and ankle trajectories obtained from the FlexPLI+SUBP and the aPLI are similar to those obtained from the PMHSs for the three buck configurations. For all buck configurations, the vertical displacements of the FlexPLI greatly differed from the vertical displacements of the FlexPLI+SUBP, the aPLI models, and the PMHS corridors.

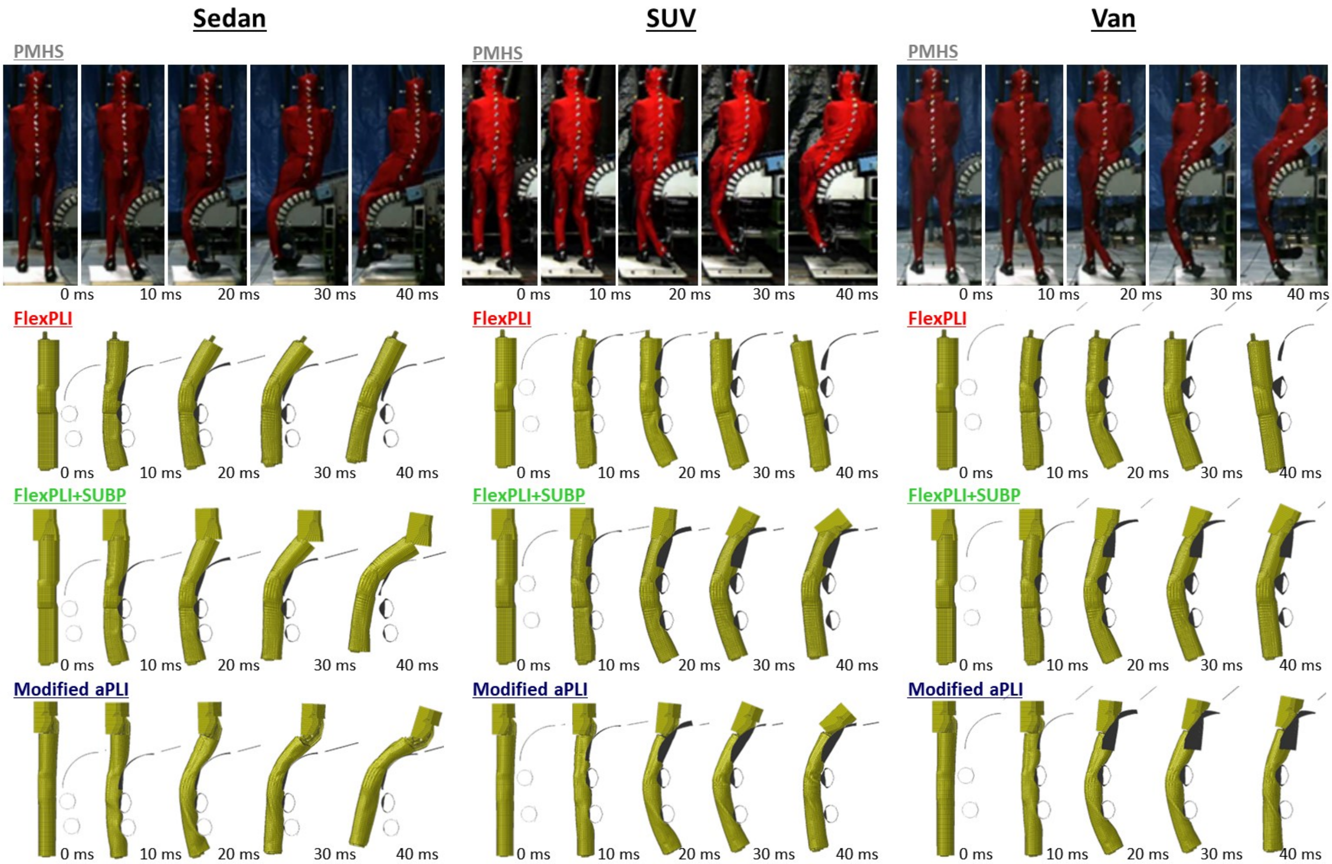

Fig. 4. In-crash kinematics for a lateral impact with a simplified Sedan (left), an SUV (middle), and a Van (right) buck configuration for the PMHS [12] and for three impactor models.

Fig. 5 shows a comparison between the PMHS contact force corridors [12] and the impactor force for three buck components (i.e., BLE, BP, and SP). Regarding the shape of the contact force corridors, it should be noted that the PMHS corridors included the contact with both the struck side (right) and the contralateral (left) lower limb, whereas the impactor only represents the lower limb of the struck side. Hence, the sequential comparison is only meaningful up to a few milliseconds after the first peak has been reached, after which the contralateral lower limb of the PMHS largely contributes to the recorded forces. Regarding the time frame of interest, particularly for the SUV and Van buck configurations, the contact forces between the FlexPLI and the BLE result in lower values than those of the PMHS tests, whereas the contact forces with the BP and SP parts result in higher values (Fig. 5, middle and right columns). Regarding the FlexPLI+SUBP, the BLE forces are higher than those of the FlexPLI and are closer to those of the PMHS corridors, particularly for the SUV and Van configurations; conversely, the values of the BP and SP forces remain high and dissimilar from those of the PMHS corridors. The aPLI results in a simultaneous increase in the BLE forces and a decrease in the BP and SP forces, providing a distribution of forces that approximate that of the PMHS corridors for the three components and the three buck configurations, simultaneously.

Fig. 6 shows the CORA scores resulting from the evaluation of the contact force responses, which were presented in Fig. 5 up to 5 ms after the first peak was reached. For all cases, their highest values correspond to those of the aPLI, which indicates an objective biofidelity improvement with respect to the PMHS data for the contact forces considered.

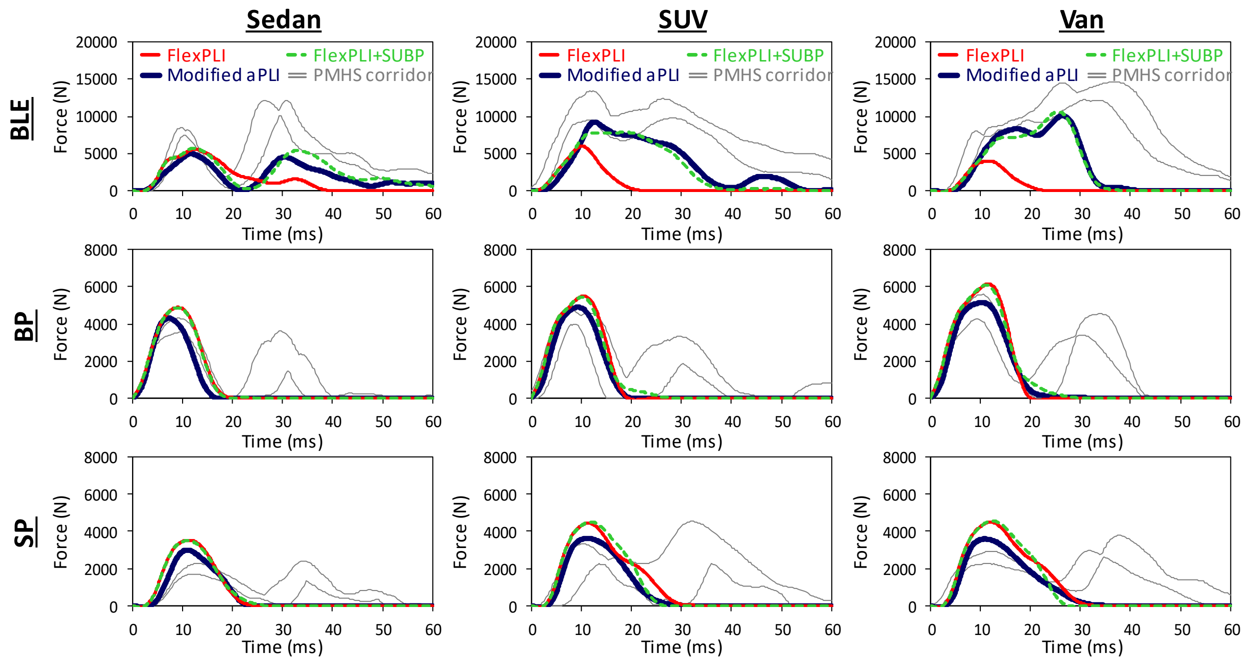

Fig. 5. PMHS test corridors [12] and simulated impactor responses for the BLE, BP, and SP contact forces for the Sedan (left column), SUV (middle column), and Van (right column) buck configurations.

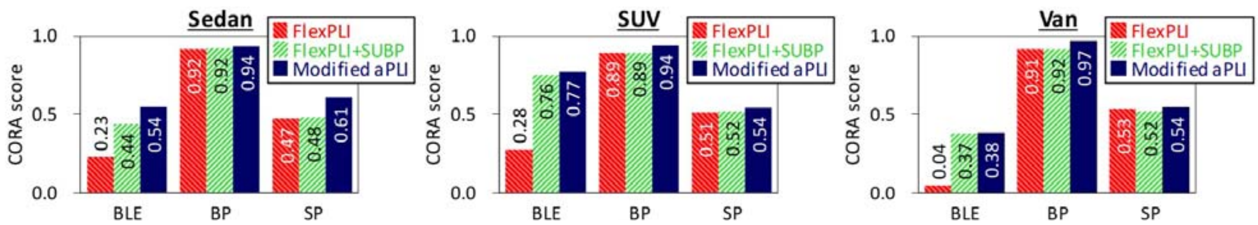

Fig. 6. CORA scores for each buck component (i.e., BLE, BP, and SP); comparison of contact forces between each of the legform impactor models (FlexPLI, FlexPLI+SUBP, and aPLI) and the PMHS.

Evaluation of the Injury Assessment Capability using the HBM Lateral and Oblique Impact Simulations

The corresponding ACL elongation responses obtained from the impact simulations are shown in Fig D19 in Appendix D. In general, the sustained ACL elongations of the Modified aPLI are closer to those of the HBM, confirming the validity of the condyle shape modification.

A comparison of the sequential images from the lateral impact simulations with the HBM and the three legform impactors using a car front-end model with a high bumper (SUV01 in Table C2, Appendix C) is presented in Fig. 7. The corresponding injury measure responses (thigh bending moments in three locations, leg bending moments in four locations, and MCL, ACL, and PCL elongations), which were obtained from the impact simulations presented in Fig. 7, are shown in Fig. 8. The overall kinematics response of the FlexPLI greatly differs from that of the HBM, resulting in low values in terms of thigh injury, early leg unloading, and early and low ligament elongation peaks (indicated by the red circles in the second row in Fig. 8). The FlexPLI+SUBP resulted in a general response that was closer to that of the HBM model; however, the thigh peak values and the leg injury values (highlighted in the third row in Fig. 8) were underestimated. The aPLI closely approximates the HBM responses, including thigh and leg injury measurement responses and peaks.

Fig. 9 enables a comparison of sequential images obtained from simulations of the lateral impact with a low-bumper car front-end model (Sedan01 in Table C2, Appendix C) for the HBM and for the three impactor models. Fig. 10 shows the injury measurement responses obtained from the same simulations. The FlexPLI+SUBP model yields a response that is close to that of the HBM, with two exceptions: an overestimation of the tibia loading in the rebound phase, and negative ACL and PCL elongation values at the beginning of the simulation. The aPLI results in a response similar to that of the HBM for both the tibia injury measures in the rebound phase and the ACL/PCL elongation modes.

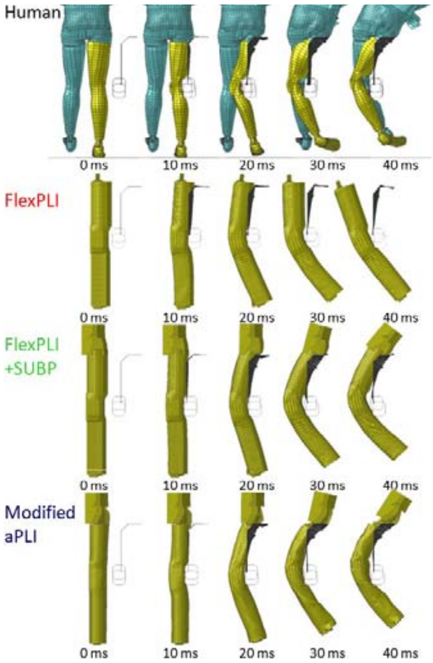

Fig. 7. In-crash kinematics of the HBM and impactor models; impact with a simplified SUV model.

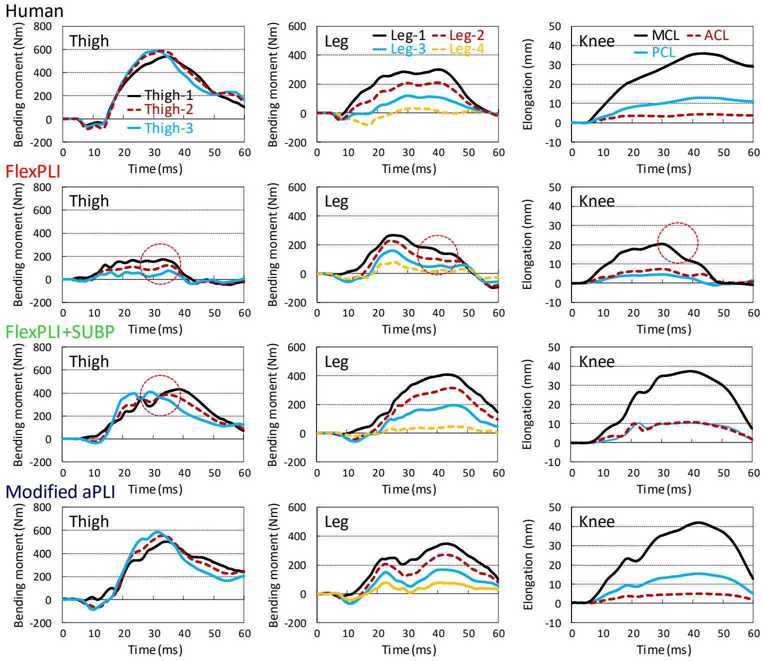

Fig. 8. Injury measurement simulated responses in a lateral impact with a simplified SUV model for the HBM (top row), FlexPLI (second row), FlexPLI+SUBP (third row), and aPLI (fourth row) models.

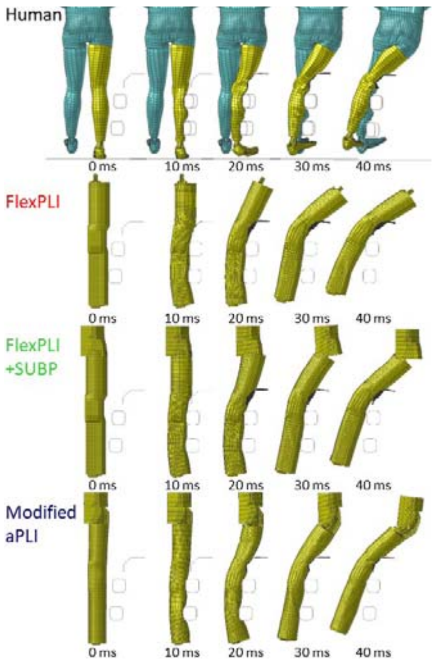

Fig. 9. In-crash kinematics of the HBM and impactor models; impact with a simplified Sedan model.

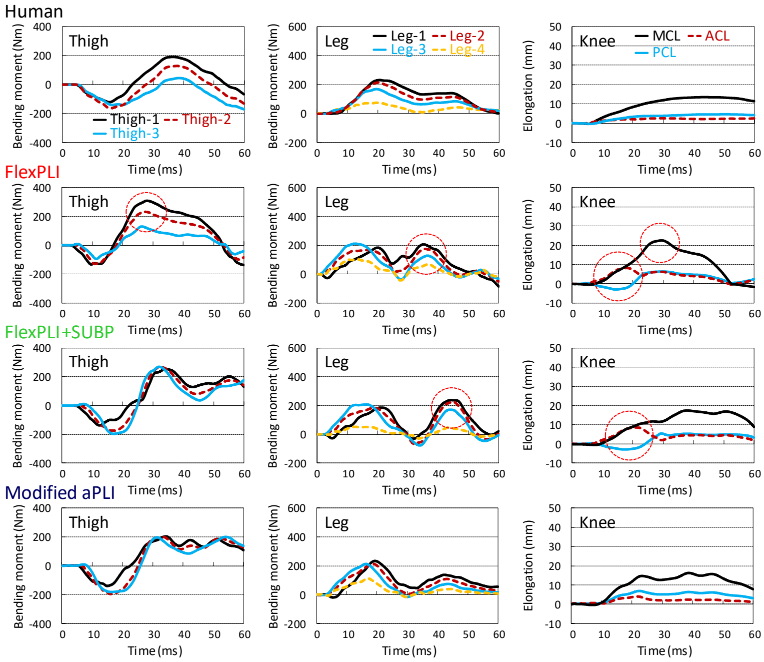

Fig. 10. Injury measurement simulated responses in a lateral impact with a simplified Sedan model for the HBM (top row), FlexPLI (second row), FlexPLI+SUBP (third row), and aPLI (fourth row) models.

Fig. 11 and Fig. 12 illustrate the CORA scores between the injury measurements obtained from simulations with the HBM and those obtained from each of the three legform impactor models in simulated lateral and oblique impacts for low- and high-bumper vehicles, respectively. The CORA scores for the aPLI reached their highest value in both vehicle groups for nearly all injury measurements.

Fig. 13 depicts the linear regression results for each of the three impactor models and the HBM for all lateral and oblique impacts with the 36 simplified car models. When compared with the values obtained from the FlexPLI (top row), all FlexPLI+SUBP (middle row) coefficient of determination (R^2) values increase and all the slope values approach the unit value. The aPLI yielded a further increase in the R^2 values; the slope values approach the unit value in terms of the peak thigh bending moment (R^2 = 0.87, slope = 0.74) and peak PCL elongation (R^2 = 0.88, slope = 0.97) compared with the corresponding FlexPLI+SUBP values. Regarding the tibia (R^2 = 0.56, slope = 0.95) and the MCL (R^2 = 0.90, slope = 1.13), the aPLI produced values in the vicinity of those obtained from the FlexPLI+SUBP model. None of the impactors resulted in high R^2 values or slope values that approached the unit value for the ACL injury measurements; however, the peak values obtained from the aPLI were significantly lower (2 to 7 mm) than those obtained from the FlexPLI and the FlexPLI+SUBP (5 to 15 mm).

Fig. 11. CORA scores for the comparison of lower-limb injury measures between each legform impactor model and the HBM in lateral and oblique impacts with low-bumper cars.

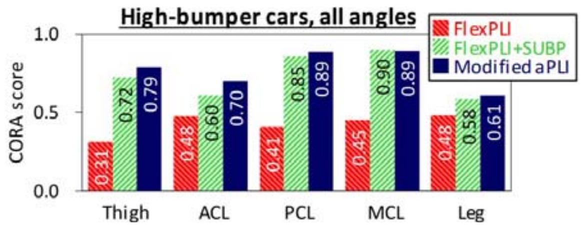

Fig. 12. CORA scores for the comparison of lower-limb injury measures between each legform impactor model and the HBM in lateral and oblique impacts with high-bumper cars.

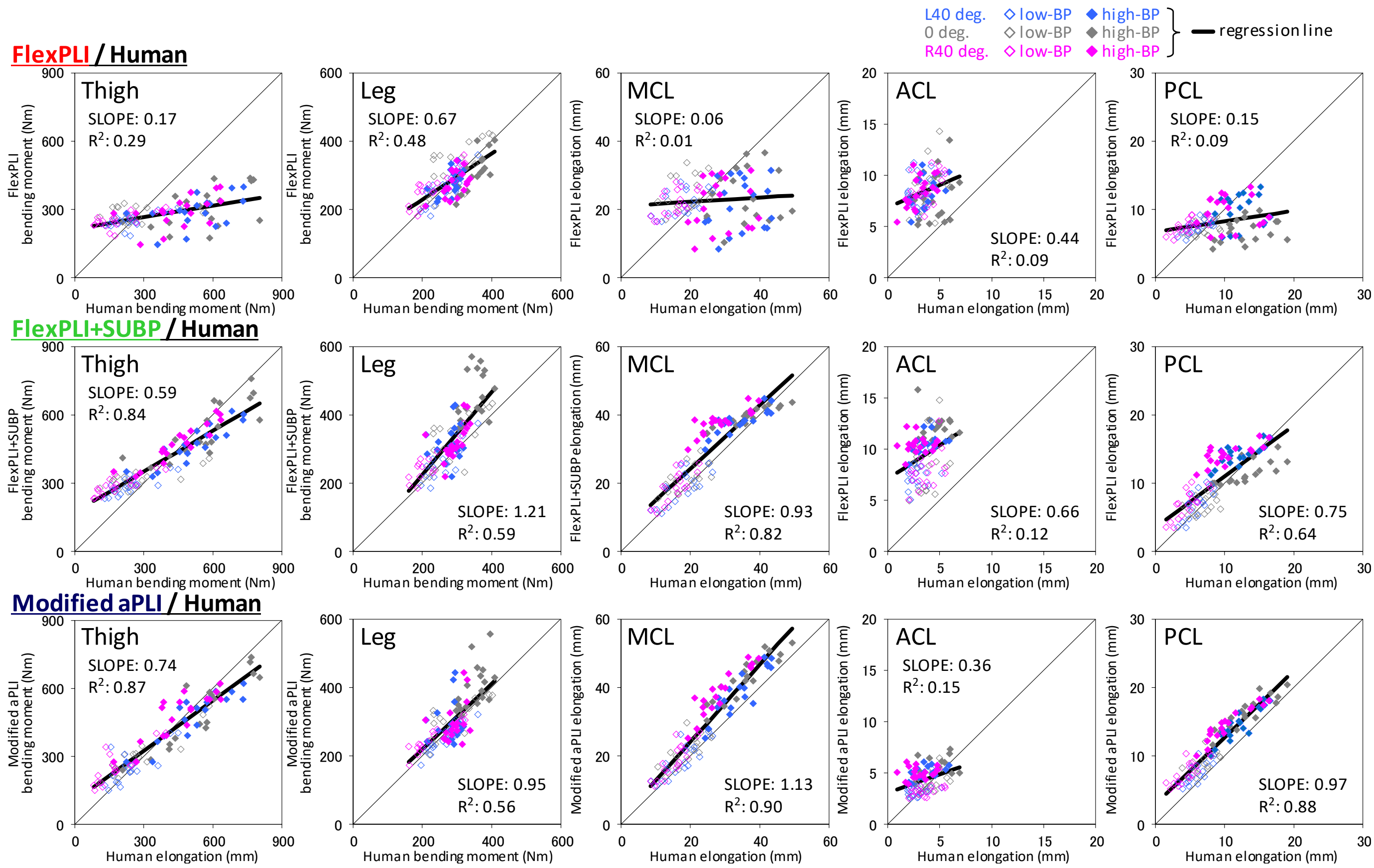

Fig. 13. Linear regression results for the peak thigh bending moment, the leg bending moment, and the MCL, ACL, and PCL elongation values obtained from simulations using the HBM, FlexPLI (top row), FlexPLI+SUBP (middle row), and aPLI (bottom row) models.

IV. DISCUSSION

The response of the impactor in terms of the distribution of forces between the impactor and each of the three main vehicle front-end components was improved because both the relative flesh-to-bone mass distribution and the mass distribution along the five sections of the mechanical lower limb are closer to those of humans. The SUBP alone increased the leading-edge force of the bonnet to levels that were similar to the PMHS force for the SUV and Van buck configurations; however, this increase was not accompanied by a corresponding decrease in the bumper and spoiler forces (red and green lines in Fig. 5). The distribution of forces was simultaneously improved for the three car front-end parts (blue lines in Fig. 5) only when human-like changes in the mass distribution were implemented for the lower limb, in addition to being implemented for the SUBP. To the best of our knowledge, this is the first study in which the response of a legform impactor is compared with contact force corridors that have been developed from PMHS tests. The comparison enabled the improvement of load distributions, which can aid vehicle designers in adopting detailed safety measures that account for the loads that are transferred between the different parts of the car front-end and the impactor in aPLI tests.

It is necessary to utilize specific aPLI structural design considerations for the knee to account for the complex three-dimensional knee kinematics that occur in oblique impacts and to capture the corresponding knee ligament injury elongations. Fig. 14 illustrates a comparison of the knee kinematics and ligament elongation simulated responses in the simulated oblique impacts between a Sedan front-end model for the HBM, the FlexPLI+SUBP (using the same knee as the one used in the FlexPLI), and the aPLI (using the redesigned knee). Under this kinematics, all three ligaments (MCL, ACL, and PCL) sustained positive elongations to different extents from an early stage of the impact. Under similar impact conditions with those of the FlexPLI+SUBP, the knee ligaments sustained a sudden peak at approximately 25 ms, which was not observed using the HBM. This peak was caused by an artefact contact between the knee condyle parts (Fig. 14, middle row) and did not occur in the aPLI knee design because the aPLI knee design eliminated the artificial contact by enabling knee rotation in the angled impacts (Fig. 14, bottom row). In addition, this phenomenon explains why the peak ACL elongation values were significantly higher for the FlexPLI and FlexPLI+SUBP models than for the HBM and why they were concentrated at the upper left part of the linear regression plots presented in Fig. 13 (fourth column). Therefore, this result highlights the importance of the aPLI knee redesign in accounting for oblique impacts.

The knee kinematics response and the ligament elongations depend on the impact angle and are non-symmetric. Regardless of the removal of the ACL artefact by redesigning the aPLI knee structure, the resulting R^2 values between the aPLI and the HBM injury measures were high and the slope values approached the unit value for all indicators (thigh, leg, MCL, and PCL), except for the ACL elongation. This was caused by the asymmetry in the HBM lower-leg anatomy in contrast to the symmetric aPLI, in combination with the narrow range of ACL elongations that were obtained under the impact conditions that were investigated in the present study. More specifically, in the cases in which the HBM right leg was impacted with an angle corresponding to the left bumper corner, the contact between the bumper and the human model was initiated from the tibia (Fig. 14, left side of the top row). Conversely, in the simulations addressing impacts to the right leg with the right bumper corner, the first contact between the bumper and the leg occurred at the head of the fibula (Fig. 14, right side of the top row). This early contact induced an early and increased horizontal displacement of the fibula and the tibia, which explains the increased ACL elongation for the right bumper corners compared with the left bumper corner. Because the aPLI has a symmetric design (and response) and has no fibula, when linear regression is applied to all angles together between the impactors and the HBM, the results show low regression values only for the ACL. When the results were analysed separately according to the impact angle (Appendix F), the R^2 and slope values for the ACL injury indicator improved for the left bumper corner and the straight bumper; however, they did not improve for the right-bumper corner angulations. This phenomenon may have been exaggerated because of the rigidity of the bumper of the simplified car front-end models, in contrast to real car front-end components, which tend to deform when they come into contact with the lower limb. In any case, despite the improvements for the left and the central impacts, the obtained values (R^2 of 0.29 and 0.25 and slope values of 0.54 and 0.59, respectively) did not indicate high injury assessment capability. The reason for this is the concentration of the ACL elongation values at very low levels and within very small ranges for all simulated conditions (1–7 mm range compared with the 9–50 mm and 1–20 mm ranges obtained for the MCL and PCL elongations, respectively). Therefore, future work shall verify whether the right-bumper corner ACL elongation asymmetric mechanism found is mitigated for impacts with real car front-end parts, as these parts tend to deform locally in contact with the head protuberance of the HBM fibula. In addition, to better understand the ACL injury assessment capability, impact conditions that produce a range of ACL elongations that are wider than those obtained in the present study shall be incorporated. Nevertheless, the aPLI presented a performance improvement compared with previous impactors for all injury measures that were analysed in the present study and for a wide range of bumper heights and angulations.

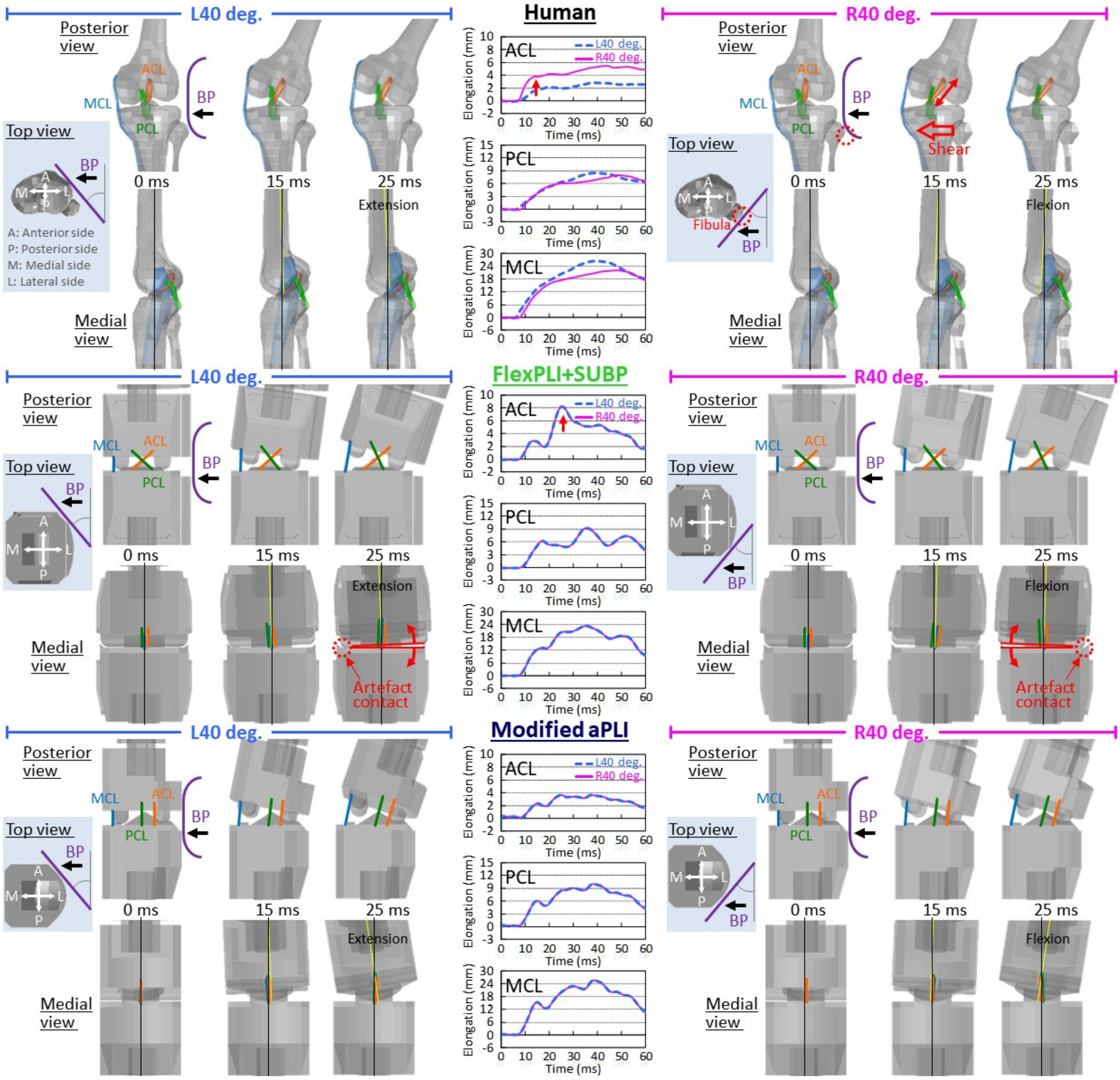

Fig. 14. Posterior view of knee kinematics and knee ligament elongation responses for simulated oblique left and right impacts with a Sedan model for the HBM (top row), the FlexPLI+SUBP model (middle row), and the aPLI model (bottom row).

V. CONCLUSIONS

In this study, the validation of the biofidelity and the injury assessment capability of the aPLI FE model were expanded by comparing the simulated response of the model with an existing set of PMHS lateral impact tests and with a new series of HBM lateral and oblique impact simulations, respectively. The improved mass distribution proved to be critical for the reproduction of biofidelic interactions with various vehicle front-end components in a manner similar to that in the PMHS lateral impacts. The structural redesign of the knee enhanced the performance of the injury assessment capability of the aPLI in oblique impacts. In the present study, the aPLI was shown to improve the performance of previous impactors over a wide range of vehicle front-end characteristics, including a wide range of bumper heights and bumper impact locations, as well as oblique impact scenarios.

VI. ACKNOWLEDGEMENTS

We would like to sincerely thank Eric Song et al. for providing the PMHS test data that were used in this study [12].

VII. REFERENCES

[1] Simms CK, Wood D, and Fredriksson R. Accidental Injury. pages 721-753, *Springer*, New York, 2015.

[2] Mizuno Y. Summary of IHRA Pedestrian Safety WG Activities (2005)-Proposed test methods to evaluate pedestrian protection afforded by passenger cars. *Proceedings of 19th ESV Conference*, 2005, Washington DC, USA.

[3] Mallory A, Fredriksson R, Rosén E, and Donnelly B. Pedestrian injuries by source: serious and disabling injuries in US and European cases. *Proceedings of Association for the Advancement of Automotive Medicine*, 2012, Seattle, USA.

[4] ITARDA. "Traffic Accident Statistics 2016 (in Japanese)" Internet: http://www.itarda.or.jp/, Cited 2018 May 15.

[5] Kikuchi Y, Takahashi Y, and Mori F. Full-scale validation of a human FE model for the pelvis and lower limb of a pedestrian. 2008, SAE Technical Paper 2008-01-1243.

[6] Carroll J, Barrow A, Hardy B, and Robinson B. Pedestrian legform test area assessment. *TRL Project Report RPN2770, Wokingham, Berkshire, UK, TRL*, 2014.

[7] Kerrigan JR, Arregui-Dalmases C, Foster J, Crandall JR, and Rizzo A. Pedestrian injury analysis: field data vs. laboratory experiments. *Proceedings of IRCOBI Conference*, 2012, Dublin, Ireland.

[8] Isshiki T, Konosu A, and Takahashi Y. Development and Evaluation of the Advanced Pedestrian Legform Impactor Prototype which can be Applicable to All Types of Vehicles Regardless of Bumper Height - Part 1: Finite Element Model. *Proceedings of IRCOBI Conference*, 2016, Malaga, Spain.

[9] Konosu A, Isshiki T, and Takahashi Y. Development and Evaluation of the Advanced Pedestrian Legform Impactor Prototype Which Can be Applicable to All Types of Vehicles Regardless of Bumper Height-Part 2: Actual Test Tool. *Proceedings of IRCOBI Conference*, 2016, Malaga, Spain.

[10] Isshiki T, Antona-Makoshi J, Atsuhiro K, and Takahashi Y. Optimal Specifications for the Advanced Pedestrian Legform Impactor. *Stapp Car Crash Journal*, 2017, 61: p. 373-395.

[11] Isshiki T, Antona-Makoshi J, Konosu A, and Takahashi Y. Simplifying the structural design of the Advanced Pedestrian Legform Impactor for use in standardized testing. 2018, SAE Technical Paper 2018-01-1049.

[12] Song E, Petit P, et al. New Reference PMHS Tests to Assess Whole-Body Pedestrian Impact Using a Simplified Generic Vehicle Front-End. *Stapp Car Crash Journal*, 2017, 61: p. 299-353.

[13] Forman JL, Joodaki H, et al. Whole-body response for pedestrian impact with a generic sedan buck. *Stapp Car Crash Journal*, 2015, 59: p. 401-444.

[14] UN. Addendum 126: Regulation No. 127 - 01 series of amendments to the regulation. 2015.

[15] Konosu A, Issiki T, Tanahashi M, and Suzuki H. Development of a biofidelic flexible pedestrian legform impactor type GT (Flex-GT). *Proceedings of 20th ESV Conference*, 2007, Lyon, France.

[16] Konosu A, Issiki T, et al. Development of a Biofidelic Flexible Pedestrian Legform Impactor Type GTR Prototype Part 1: Development and Technical Evaluations. *Proceedings of 21st ESV Conference*, 2009, Stuttgart, Germany.

[17] Been B, Burleigh M, Konosu A, Issiki T, Takahashi Y, and Suzuki H. Development of a Biofidelic Flexible Pedestrian Legform Impactor Type GTR prototype, Part 2: Technical Details. *Proceedings of 21th ESV Conference*, 2009, Stuttgart, Germany.

[18] Gehre C, Gades H, and Wernicke P. Objective rating of signals using test and simulation responses. *Proceedings of 21st ESV Conference*, 2009, Stuttgart, Germany.

[19] Takahashi Y, Kikuchi Y, Mori F, and Konosu A. Advanced FE lower limb model for pedestrians. *Proceedings of 18th ESV Conference*, 2003, Nagoya, Japan.

[20] Kikuchi Y, Takahashi Y, and Mori F. Development of a finite element model for a pedestrian pelvis and lower limb. 2006, SAE Technical Paper 2006-01-0683.

[21] Takahashi Y, Suzuki S, Ikeda M, and Gunji Y. Investigation on pedestrian pelvis loading mechanisms using finite element simulations. *Proceedings of IRCOBI Conference*, 2010, Hanover, Germany.

[22] Isshiki T, Konosu A, and Takahashi Y. Development of an Appropriate Pedestrian Legform Impact Test Method which can be used for all Types of Vehicles including High Bumper Vehicles-Development of a Simplified Upper Body Part (SUBP) FE Model. *Proceedings of IRCOBI Conference*, 2014, Berlin, Germany.

[23] Kerrigan JR, Bhalla KS, Madeley NJ, Funk JR, Bose D, and Crandall JR. Experiments for establishing pedestrian-impact lower limb injury criteria. 2003, SAE Technical Paper 2003-01-0895.

[24] Bose D, Bhalla K, Rooij L, Millington S, Studley A, and Crandall J. Response of the knee joint to the pedestrian impact loading environment. 2004, SAE Technical Paper 2004-01-1608.

[25] Kerrigan J, Subit D, Untaroiu C, Crandall J, and Rudd R. Pedestrian lower extremity response and injury: A small sedan vs. a large sport utility vehicle. *SAE International Journal of Passenger Cars-Mechanical Systems*, 2008, 1(2008-01-1245): p. 985-1002.

APPENDIX A: IMPACTOR FINITE ELEMENT MODELS

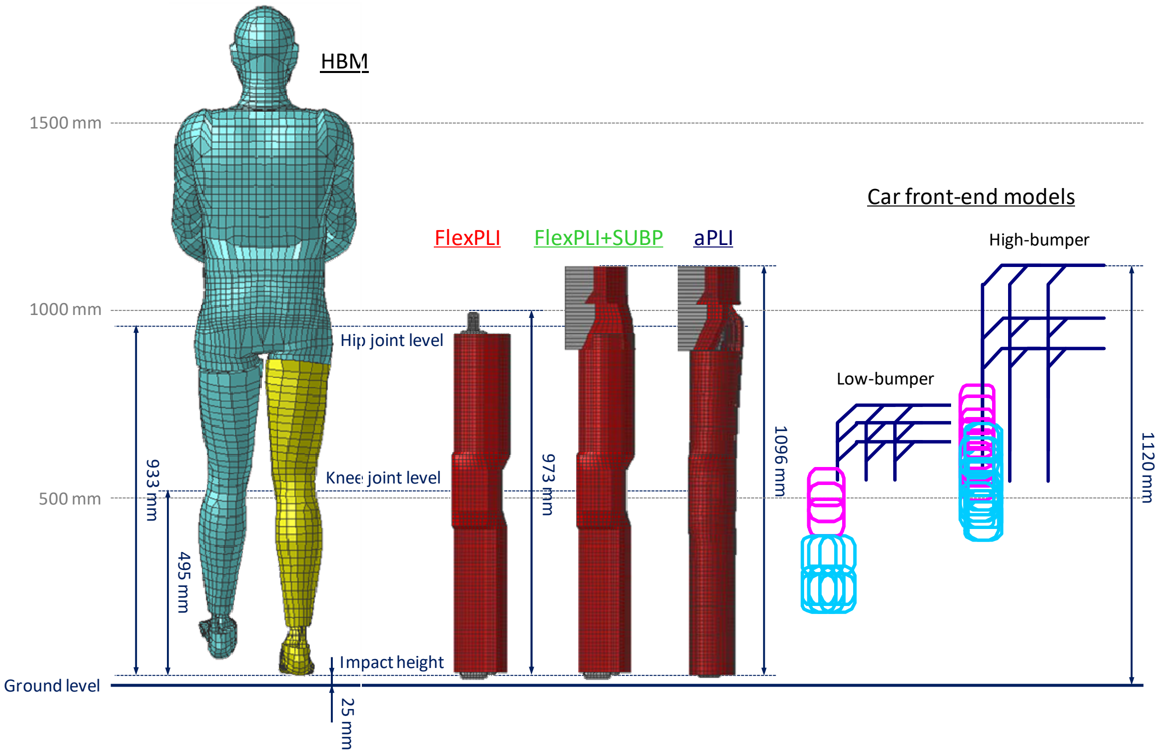

Fig. A15. An HBM, three legform impactor models, and 36 simplified model configurations of car front-ends.

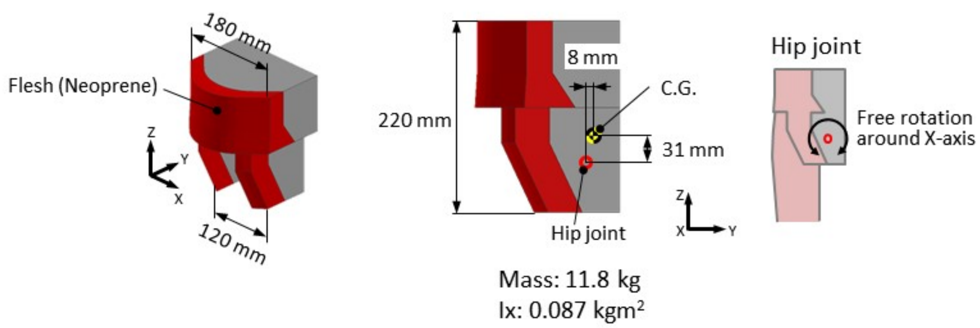

Fig. A16. SUBP technical specifications.

APPENDIX B: HUMAN BODY MODEL

An HBM that has been previously validated at both component- and full-scale levels [5][19-21] with a great amount of PMHS experimental data was incorporated into the present study. Details on the model validation under dynamic conditions that are most relevant to this study are provided in the original publications [5][19-21], and are briefly discussed in the present study. The component validations included the lateral compression of the pelvis; the lateral three-point bending of the thigh, leg, femur, tibia, and fibula; the tension of the individual knee ligaments; and three- and four-point bending of the knee. The force-deflection and moment-deflection responses of the femur, tibia, and fibula bone models until the occurrence of fractures were validated based on simulations [19-20] via three-point bending tests at three different loading locations for each bone [23]. The knee ligament force-displacement response until rupture was validated based on simulations [19-20] of dynamic ligament tensile tests [24]. The bending angle response of the bending moment of the assembled knee was validated by means of simulations [20] of the lateral three- and four-point valgus bending tests [24]. At the full scale, the trajectories of the head, the first and the eighth thoracic vertebrae, and the pelvis were validated by simulating [5] full-scale PMHS impact tests, in which small Sedan and SUV cars were used [25]. Under these conditions, the model predicted the general injury trends that had been observed in the experiments, including the presence of pelvis fractures and knee-ligament ruptures and the absence of tibia and femur fractures [5].

APPENDIX C: SIMPLIFIED CAR FRONT-END MODELS

A set of 36 simplified models of car front-ends was adopted from a previous aPLI work [11][22]. The car models included simplified BLE, BP, and SP components, whose relative layout and structural properties were defined based on a wide range of commercial Sedans and SUVs from Europe, Japan, and the US [2]. The BP and the SP were modelled as rigid bodies that were connected to a node through simplified joint elements, for which the force-deflection characteristics were defined along the longitudinal direction of the car. The BLE was modelled with deformable shell elements, which represented a sheet structure made of steel. Both of the lateral ends of the BLE were rigidly connected to the node that represented the mass of a car. Fig. C17 shows a schematic of the general construction of the simplified car models, an overview of the geometrical characteristics of the car models, and a sample of the force displacement characteristics applied to the BP and SP joint elements. Detailed information for each of the 36 models is provided in Table C1 and Table C2 as well.

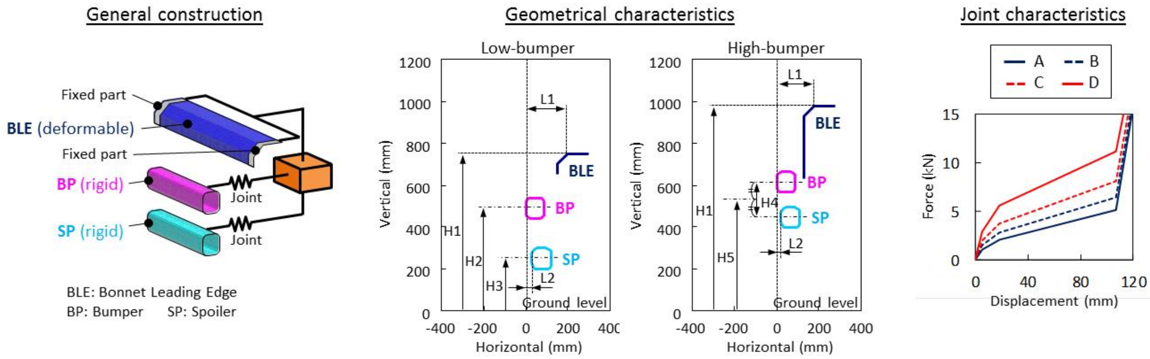

Fig. C17. General construction of the simplified car front-end models (left), general geometric characteristics (middle), and BP and SP joint characteristics (right)

TABLE C1 VARIABLE PARAMETERS AND LEVELS FOR THE SIMPLIFIED CAR FRONT-END MODELS

High-bumper

	Parameter	Unit	Level 1	Level 2	Level 3
K1	BLE thickness	mm	0.4	0.6	-
K2	BP stiffness	-	B	C	D
K3	SP stiffness	-	A	C	D
H1	BLE height	mm	900	980	1120
H4	BP height - SP height	mm	40	110	170
H5	Average height of BP and SP	mm	530	580	670
L1	BLE lead	mm	110	180	280
L2	SP lead	mm	0	10	20

Low-bumper

	Parameter	Unit	Level 1	Level 2	Level 3
K1	BLE thickness	mm	0.4	0.6	-
K2	BP stiffness	-	B	C	D
K3	SP stiffness	-	A	C	D
H1	BLE height	mm	650	700	750
H2	BP height	mm	450	490	530
H3	SP height	mm	250	270	350
L1	BLE lead	mm	125	200	275
L2	SP lead	mm	-20	0	30

TABLE C2

GEOMETRIC AND MECHANICAL PROPERTIES OF THE SIMPLIFIED CAR FRONT-END MODELS

High-bumper

ID	K1	K2	K3	H1	H4	H5	L1	L2
SUV01	0.4	B	A	900	40	530	110	0
SUV02	0.4	B	C	980	110	580	180	10
SUV03	0.4	B	D	1120	170	670	280	20
SUV04	0.4	C	A	900	110	580	280	20
SUV05	0.4	C	C	980	170	670	110	0
SUV06	0.4	C	D	1120	40	530	180	10
SUV07	0.4	D	A	980	40	670	180	20
SUV08	0.4	D	C	1120	110	530	280	0
SUV09	0.4	D	D	900	170	580	110	10
SUV10	0.6	B	A	1120	170	580	180	0
SUV11	0.6	B	C	900	40	670	280	10
SUV12	0.6	B	D	980	110	530	110	20
SUV13	0.6	C	A	980	170	530	280	10
SUV14	0.6	C	C	1120	40	580	110	20
SUV15	0.6	C	D	900	110	670	180	0
SUV16	0.6	D	A	1120	110	670	110	10
SUV17	0.6	D	C	900	170	530	180	20
SUV18	0.6	D	D	980	40	580	280	0

Low-bumper

ID	K1	K2	K3	H1	H2	H3	L1	L2
Sedan01	0.4	B	A	650	450	250	125	-20
Sedan02	0.4	B	C	700	490	270	200	0
Sedan03	0.4	B	D	750	530	350	275	30
Sedan04	0.4	C	A	650	490	270	275	30
Sedan05	0.4	C	C	700	530	350	125	-20
Sedan06	0.4	C	D	750	450	250	200	0
Sedan07	0.4	D	A	700	450	350	200	30
Sedan08	0.4	D	C	750	490	250	275	-20
Sedan09	0.4	D	D	650	530	270	125	0
Sedan10	0.6	B	A	750	530	270	200	-20
Sedan11	0.6	B	C	650	450	350	275	0
Sedan12	0.6	B	D	700	490	250	125	30
Sedan13	0.6	C	A	700	530	250	275	0
Sedan14	0.6	C	C	750	450	270	125	30
Sedan15	0.6	C	D	650	490	350	200	-20
Sedan16	0.6	D	A	750	490	350	125	0
Sedan17	0.6	D	C	650	530	250	200	30
Sedan18	0.6	D	D	700	450	270	275	-20

APPENDIX D: EFFECTIVENESS OF MODIFICATIONS

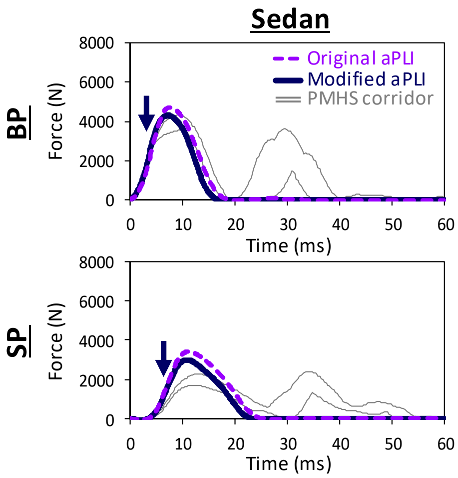

Fig. D18. Effect of mass distribution modification on the impact force with respect to the PMHS response in lateral impact tests.

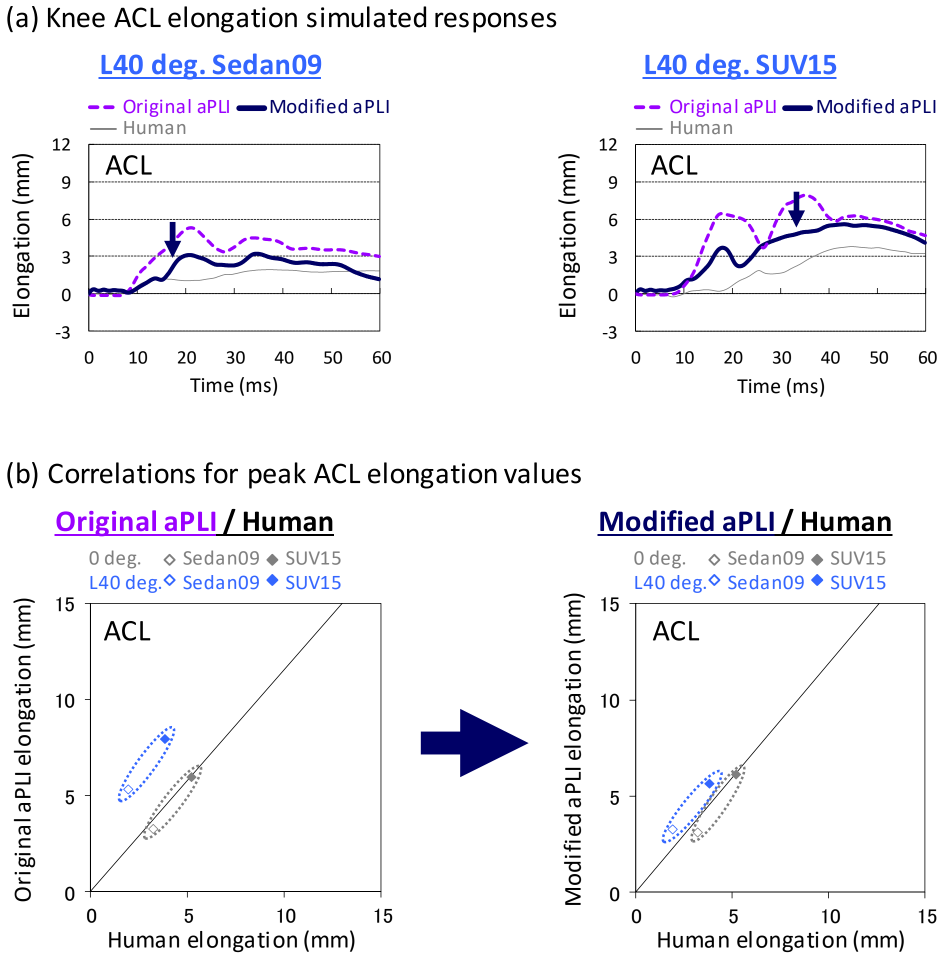

Fig. D19. Effect of the modification of the knee condyle shape on the ACL elongation with respect to the HBM response in lateral and oblique impact simulations

Appendix E: PMHS test corridors and simulated impactor response for knee and ankle trajectories

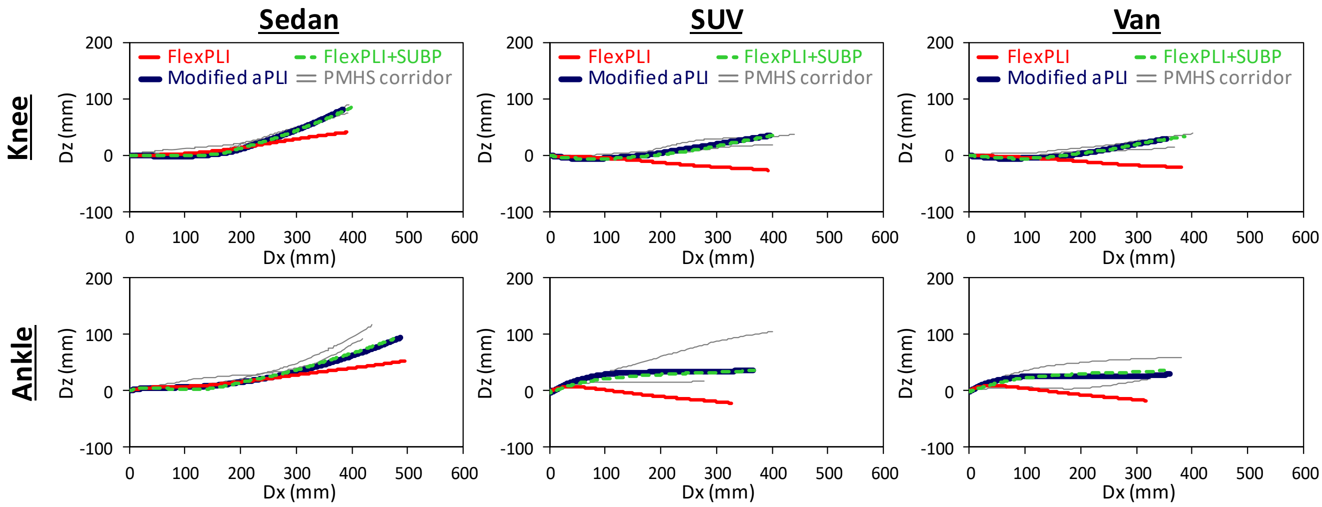

Fig. E20. PMHS test corridors [12] and the response of simulated impactors for knee and ankle trajectories for the Sedan (left column), SUV (middle column), and Van (right column) buck configurations

APPENDIX F: LINEAR REGRESSION RESULTS FOR ANTERIOR CRUCIATE LIGAMENT ELONGATION MEASUREMENTS

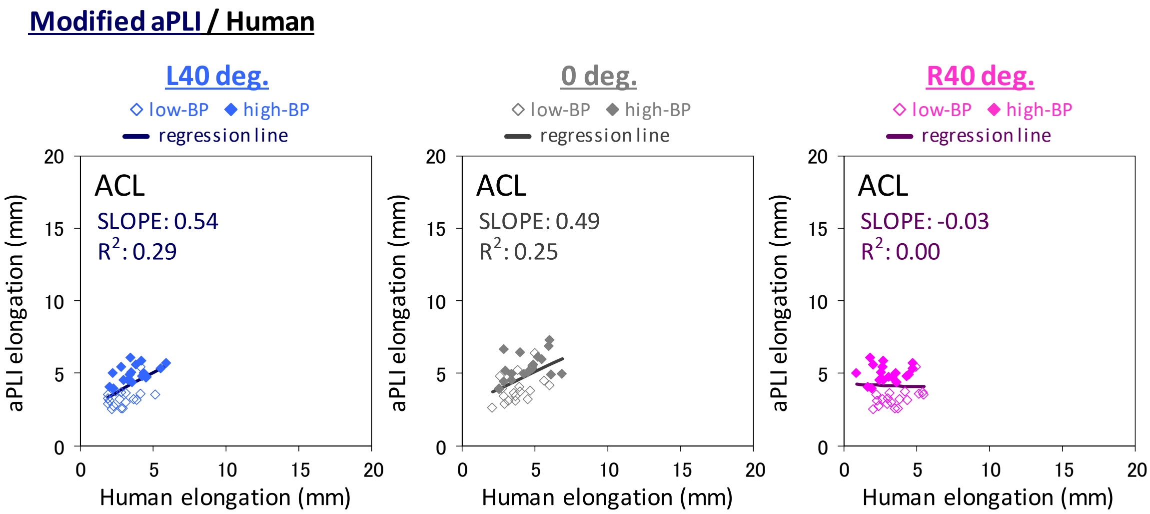

Fig. F21. Linear regression for peak ACL elongation values between simulations with the HBM and simulations with the aPLI impactor model for impact conditions of the left bumper corner (left), the straight bumper (middle), and the right bumper corner (right).